complex to the singlet primary geminate pair (^{1}PGP). Although the electron may have enough energy to dissociate to the singlet secondary geminate pair (^{1}SGP), it must first traverse an energy barrier that is affected by the solvent dielectric and transport properties. Since recent evidence shows that electrons move through water by a Grotthus mechanism,[36] influences that disrupt the structure of water, such as a highly ionic medium, would inhibit the mobility of electrons to form the ^{1}SGP, increasing the likelihood of decay either to the triplet state (intersystem crossing), resulting in luminescence, or back to the ground-state energy curve (primary pair recombination). Once the ^{1}SGP is reached, the previously observed[11] reactive-scavenging kinetics, which includes secondary pair recombination, half-order hydronium ion scavenging, and hydrated electrons escaping secondary recombination or scavenging, becomes operative. Apparently, such a reactive-scavenging kinetic scheme is not observed for hydronium ion quenching of the luminescence probably because the lifetime of the triplet state is long enough to permit the slower conventional second-order kinetics observed.

Acknowledgment. This research was supported by the donors of the Petroleum Research Fund, administered by the American Chemical Society. The authors also thank Clifford Kubiak and Fred Lemke, Department of Chemistry, Purdue University, for their kind assistance and use of their equipment in measuring the luminescence lifetimes.

Registry No. $CuCl_2^-$, 15697-16-2; $CuCl_3^{2-}$, 29931-61-1; Cl^-, 16887-00-6; H^+, 21408-02-5; H_2, 1333-74-0.

(36) Hameka, H. F.; Robinson, G. W.; Marsden, C. J. *J. Phys. Chem.* **1987**, *91*, 3150.

Contribution from the Department of Chemistry, North Dakota State University, Fargo, North Dakota 58105

Rotational Strengths of Sharp-Line Electronic Transitions of Tris(ethylenediamine)chromium(III)

Patrick E. Hoggard

Received April 14, 1988

A method has been developed to calculate relative rotational strengths for transition-metal complexes based on the actual geometry of the ligating atoms and any other atoms contributing to the molecular dissymmetry. Such calculations are particularly useful in the analysis of sharp-line phenomena in circular dichroism spectra, since narrow CD peaks often represent single, nondegenerate electronic transitions. This approach was used to examine a controversy over the splitting of the $^2T_{1g}$ components in $[Cr(en)_3]^{3+}$ arising from quite different assignments in single-crystal and solution spectra. Calculations suggest that both assignments are correct. One reason for the discrepancy appears to be that the twist angle of the nitrogen coordination sphere is closer to that of an octahedron in solution than in the crystal, leading to a larger $^2T_{1g}$ splitting. The calculations also indicate that the chelate ring conformation in solution is *lel*$_2$*ob*, as it is also (predominantly) in crystalline $[Cr(en)_3]Cl_3$. The marked sensitivity of the calculated signs and magnitudes of the sharp-line CD peaks to the twist angle of the complex was instrumental in reaching these conclusions.

Introduction

In an isotropic collection of chiral molecules the rotatory strength of an electronic transition from the ground state, ψ_0, to an excited eigenstate, ψ_j, is related to the product of the electric dipole and magnetic dipole transition moments between the two states[1]

$$R(0\rightarrow j) = \mathrm{Im}[\langle\psi_0|\mathbf{Q}|\psi_j\rangle\cdot\langle\psi_j|\mathbf{M}|\psi_0\rangle] \quad (1)$$

where **Q** and **M** are the electric and magnetic dipole operators, respectively. Im denotes the imaginary part of the complex expression. The dot indicates that the rotational strength is a pseudoscalar product, i.e., that the rotational strength depends on the cosine of the angle between the electric and magnetic moment vectors.

$$R(0\rightarrow j) = \mathrm{Im}[\langle\psi_0|Q_x|\psi_j\rangle\langle\psi_j|M_x|\psi_0\rangle + \langle\psi_0|Q_y|\psi_j\rangle\langle\psi_j|M_y|\psi_0\rangle + \langle\psi_0|Q_z|\psi_j\rangle\langle\psi_j|M_z|\psi_0\rangle] \quad (2)$$

The rotational strength is directly proportional to the area under the corresponding circular dichroism (CD) band.[2,3]

The one-electron electric dipole operator is proportional to the position vector **r**, and the magnetic dipole operator to the orbital and spin angular momenta, **l** and **s**.

$$\mathbf{Q} = e_{el}\mathbf{r} \qquad \mathbf{M} = \frac{e_{el}}{2mc}(\mathbf{l} + 2\mathbf{s}) \quad (3)$$

where m is the mass of and e_{el} is the charge on an electron.[4]

Moffitt[5] was the first to use a ligand field model to evaluate eq 2 for transition-metal complexes. There are three elements in the construction of a model to use eq 2 to calculate rotational strengths for metal complexes: how the wave functions are to be defined, and how the electric and magnetic dipole matrix elements are to be evaluated. There have been two distinct approaches to the definition of the wave functions. One is to use orbital wave functions, allowing the ready evaluation of electric and magnetic transition dipole matrices from the properties of atomic orbitals. The wave functions are then, directly or indirectly, linear combinations of multielectron atomic orbital basis functions.

The second approach is to ignore the orbital composition of the multielectron wave functions and instead to identify them by group representation labels. Electric and magnetic dipole matrices can then be constructed by means of vector coupling coefficients. This approach is only useful when the symmetry of the functions used is high and is most powerful when octahedral wave functions are employed. This takes maximum advantage of group-theoretical methods, but since electric dipole matrix elements are zero between the eigenfunctions of d^n in O_h symmetry (i.e. O_h molecules are optically inactive), a lower-symmetry field must be introduced as a perturbation.

Moffitt used, implicitly, orbital wave functions, concentrating on the one-electron transition responsible for the spin-allowed bands in Cr(III) and Co(III) complexes. The problem he then faced has remained a fundamental concern in all subsequent models. When d wave functions are used in the basis set, the magnetic moment integrals can be evaluated straightforwardly,

(1) Condon, E. U. *Rev. Mod. Phys.* **1937**, *9*, 432.
(2) Moffitt, W.; Moscowitz, A. *J. Chem. Phys.* **1959**, *30*, 648.
(3) Saito, Y. *Inorganic Molecular Dissymmetry*; Springer-Verlag: West Berlin, 1979.
(4) Griffith, J. S. *The Theory of Transition-Metal Ions*; Cambridge University Press: Cambridge, U.K., 1964, Chapter 3.
(5) Moffitt, W. *J. Chem. Phys.* **1956**, *25*, 1189.

0020-1669/88/1327-3476$01.50/0

Table I. Electric Moment Matrix Elements $\langle d_i|eQ|d_j\rangle$ in the Complex Trigonal Basis (C_3 along (1, 1, 1))[a]

	t_0	t_+	t_-	e_+	e_-
t_0	0	$(i/\sqrt{2})q_3\mathbf{k}_-$	$(-i/\sqrt{2})q_3\mathbf{k}_+$	$(i/\sqrt{2})q_0\mathbf{k}_-$	$(-i/\sqrt{2})q_0\mathbf{k}_+$
t_+	$(-i/\sqrt{2})q_3\mathbf{k}_+$	$q_4\mathbf{k}_0$	$q_5\mathbf{k}_+$	$-q_1\mathbf{k}_0$	$q_2\mathbf{k}_+$
t_-	$(i/\sqrt{2})q_3\mathbf{k}_-$	$q_5\mathbf{k}_-$	$q_4\mathbf{k}_0$	$q_2\mathbf{k}_-$	$q_1\mathbf{k}_0$
e_+	$(-i/\sqrt{2})q_0\mathbf{k}_+$	$-q_1\mathbf{k}_0$	$q_2\mathbf{k}_+$	$q_6\mathbf{k}_0$	$q_7\mathbf{k}_+$
e_-	$(i/\sqrt{2})q_0\mathbf{k}_-$	$q_2\mathbf{k}_-$	$q_1\mathbf{k}_0$	$q_7\mathbf{k}_-$	$q_6\mathbf{k}_0$

[a] $\mathbf{k}_+ = \mathbf{i} + i\mathbf{j}$; $\mathbf{k}_- = \mathbf{i} - i\mathbf{j}$; $\mathbf{k}_0 = \mathbf{k}$.

but the electric dipole elements are all zero, because the electric dipole operator has odd parity. Moffitt's solution was to allow mixing of metal d and p wave functions under the static symmetry of the dissymmetric molecule; p–d mixing can take place in several point groups but will not produce nonzero results from eq 2 except in point groups in which some corresponding components of **r** and **l** (x and l_x, etc.) transform as the same row of the same irreducible representation.

The specific problems in the evaluation of the rotational strength from eq 2 have to do with the effect of geometry. The geometry of the ligands, including the atoms not coordinating to the metal, determines the extent of dissymmetry and hence the form and degree of p–d mixing. The ligand geometry also directly influences the eigenfunctions ψ_0 and ψ_j. The need to take explicit account of geometry has been, at various levels of sophistication, at the heart of all the theoretical treatments of optical activity in transition-metal complexes since and including Moffitt's original paper, including also the development of sector rules to predict the sign of the Cotton effect for certain electronic transitions.[6]

Much of this work has centered on tris(bidentate) complexes. Moffitt's approach was to use O_h eigenfunctions and to introduce a general trigonal potential consisting of a sum of spherical harmonics transforming as A_1 in the D_3 point group of an idealized complex in order to accomplish the p–d mixing. His conclusion that certain spin-allowed d–d transitions for d^3 and d^6 complexes had net optical activity was refuted by Sugano[7] and traced to a sign error in the evaluation of the angular momentum matrix elements.[8]

Karipides and Piper, however, showed that using D_3 wave functions with Moffitt's trigonal potential did yield net optical activity that was in fair agreement with experiment, even though the net activity of the octahedral parents was zero.[9]

In a later paper[10] these same authors also showed that when the electric dipole interaction is derived from p–d mixing, the resulting $\langle d_i|\mathbf{Q}|d_j\rangle$ matrix has higher symmetry than is required in the D_3 point group. Following their example and using the complex trigonal basis of Griffith[11]

$$f_+ = \frac{-i}{\sqrt{2}}x + \frac{1}{\sqrt{2}}y$$
$$f_- = \frac{i}{\sqrt{2}}x + \frac{1}{\sqrt{2}}y \qquad (4)$$
$$f_0 = iz$$

the radial vector $\mathbf{Q} = x\mathbf{i} + y\mathbf{j} + z\mathbf{k}$ becomes

$$\mathbf{Q} = if_+\mathbf{k}_- - if_-\mathbf{k}_+ - if_0\mathbf{k}_0 \qquad (5)$$

The complex trigonal d orbitals $\{t_0, t_+, t_-, e_+, e_-\}$[10] transform as the $\{A_1, E_+, E_-, E_+, E_-\}$ components of D_3, while the coordinate functions $\{f_+, f_-, f_0\}$ transform as $\{E_+, E_-, A_2\}$. The coupling coefficients of Griffith[11] may then be used to express the elements of the $\langle d_i|e_{el}\mathbf{Q}|d_j\rangle$ matrix in terms of reduced matrix elements q_0 through q_7, of the form $e\langle d||f||d\rangle$, as shown in Table I. For example, $q_0 = e_{el}\langle t(a_1)||f(e)||e\rangle$ and $q_1 = e_{el}\langle t(e)||f(a_2)||e\rangle$.

At this point there are several options for the evaluation of the eight reduced matrix elements. If it is assumed that the primary mechanism for the acquisition of nonzero electric dipole strengths by the d orbitals derives from p–d mixing under the static symmetry, as Moffitt did, the values of all eight q_i are fixed within a constant factor.[9] Similarly, d–f mixing fixes all eight reduced matrix elements.[9] A direct quantum-mechanical calculation of the q_i may also be attempted. Piper and Karipides used this approach for the three reduced matrix elements of the type $\langle t||f||e\rangle$, using admixtures of metal and ligand wave functions and comparing the results with CD data for the spin-allowed $t \rightarrow e$ transitions.[10] In other words, d–d dipole moments are presumed to be borrowed from charge-transfer transitions. Finally, some or all of the q_i may be left as empirical parameters.

Richardson,[12] observing that ligand field treatments still predicted that the net rotational strength of the $^4A_{2g} \rightarrow {}^4T_{2g}$ transition of d^3 complexes should be zero, extended the previous approaches to include second-order perturbation contributions and differentiated between the trigonal fields caused by coordinated and noncoordinated atoms. He also considered coupled-oscillator two-electron transitions, i.e., one electric dipole-allowed oscillator on the ligand and one magnetic dipole-allowed oscillator on the metal. Richardson has also tried to estimate the extent to which vibronic perturbations (as opposed to the static field) contribute to rotational strengths, concluding that in most cases static effects ought to dominate.[13]

Schäffer was the first to bring angular overlap model (AOM) methods to bear on the problem of rotational strengths.[14] He was able to calculate transition energies as a function of trigonal distortion angles representing the approximate angular deviations from an orthoaxial arrangement of six coordinated atoms. Without an explicit evaluation of the electric dipole matrix elements, he used symmetry arguments based on the mixing of metal states with ungerade excited states by means of either the static potential or vibronic coupling.

All of the approaches discussed above were used by their authors to calculate CD spectra of spin-allowed $t \rightarrow e$ transitions, most commonly of d^3 and d^6 complexes. The problem with these is that each band (defined as a $^4A \rightarrow {}^4T$ transition in O_h notation) consists of at least two components (in the spin-free approximation) with different (but usually not much different) energies. Including spin–orbit coupling there are *six* different components. Experimental problems arise especially in the near-cancellation of oppositely signed CD peaks that are closely spaced in energy. This has provoked CD measurements on oriented single crystals in order to assign proper rotational strengths at least to the spin-free components.[15-18] The crystalline environment is, however, different from the solution environment, probably not as symmetrical, and so the conclusions from single-crystal measurements may not carry over well to solution (there is also an orientation problem, vide infra). This is particularly so because of the marked sensitivity of rotational strengths to geometric factors.

An alternative is to focus primarily on single-component transitions, for which there can be no ambiguity about the signs and magnitudes of the rotational strengths, given a correct assignment of the electronic states involved. Eight such transitions occur for d^3 complexes, all $t_2 \rightarrow t_2$ transitions, all spin-forbidden quartet–doublet transitions, and all narrow, because the excited states are geometrically very similar to the ground state. Predicting the rotational strengths of these bands is, however, more difficult than it is for the spin-allowed bands, because intensity-borrowing from spin-allowed bands through spin–orbit coupling must be considered.

(6) Mason, S. F. *Molecular Optical Activity and the Chiral Discriminations*; Cambridge University Press: Cambridge, U.K., 1982.
(7) Sugano, S. *J. Chem. Phys.* **1960**, *33*, 1883.
(8) Poulet, H. *J. Chim. Phys.* **1962**, *59*, 584.
(9) Piper, T. S.; Karipides, A. *Mol. Phys.* **1962**, *5*, 475.
(10) Karipides, A. G.; Piper, T. S. *J. Chem. Phys.* **1964**, *40*, 674.
(11) Griffith, J. S. *The Irreducible Tensor Method for Molecular Symmetry Groups*; Prentice-Hall: Englewood Cliffs, NJ, 1962.
(12) Richardson, F. S. *J. Phys. Chem.* **1971**, *75*, 692.
(13) Richardson, F. S.; Hilmes, G.; Jenkins, J. J. *Theor. Chim. Acta* **1975**, *39*, 75.
(14) Schäffer, C. E. *Proc. R. Soc. London* **1967**, *297*, 96.
(15) McCaffery, A. J.; Mason, S. F. *Mol. Phys.* **1963**, *6*, 359.
(16) Judkins, R. R.; Royer, D. J. *Inorg. Chem.* **1974**, *13*, 945.
(17) Kuroda, R.; Saito, Y. *Bull. Chem. Soc. Jpn.* **1976**, *49*, 433.
(18) Jensen, H. P.; Galsbol, F. *Inorg. Chem.* **1977**, *16*, 1294.

Early measurements of sharp-line optical rotatory dispersion or CD spectra[19-21] of Cr(III) complexes were not accompanied by attempts to predict the signs and magnitudes of the rotational strengths by means of ligand field theory. In 1973 Kaizaki, Hidaka, and Shimura[22] developed a model in which the excited t_2^3 doublet states were mixed with the $^4T_{2g}$ components $^4A_1$ and ^4E by spin–orbit coupling. By the use of vector coupling coefficients to relate the rotational strengths of the five spin–orbit components of the $^4A_{2g} \rightarrow (^2E_g, ^2T_{1g})$ transitions, these rotational strengths could be represented on a relative basis in terms of two parameters, $R(^4A_1)$ and $R(^4E)$, the rotational strengths of the two spin-free components of the $^4A_{2g} \rightarrow {}^4T_{2g}$ transition. These can in principle be measured, but the difficulties mentioned above make it more appropriate to consider them unknown or to use them as adjustable parameters. No attempt was made to evaluate $R(^4A_1)$ and $R(^4E)$ theoretically. In measurements of solution CD spectra of $[Cr(en)_3]^{3+}$ and other trigonal or approximately trigonal Cr(III) complexes these relationships and the expectation that the rotational strengths of $R(^4A_1)$ and $R(^4E)$ should have opposite signs were used to assign the three spin-forbidden bands generally seen in the CD spectra to the ^2E_g and the two trigonal components of the $^2T_{1g}$ state. This assignment pointed to a trigonal $^2T_{1g}$ splitting on the order of 300 cm^{-1}, leaving the problem of explaining this unexpectedly large splitting.

Hilmes, Brittain, and Richardson[23] examined the CD spectra of the spin-forbidden lines of $[Cr(en)_3]^{3+}$ in solution, also observing three bands near 650 nm and concurring in the assignment of these bands to the trigonal components of the $\{^2E_g, ^2T_{1g}\}$ states. Their attempt to explain the observed rotational strengths was based on eigenfunctions assigned to O_h state labels, modified by spin–orbit coupling in order to mix quartet character into the doublet functions, and a trigonal field perturbation in order to mix the ligand field quartet states with an assumed $^4T_{2u}$ excited state and to account for mixing of the O_h-labeled quartets and doublets under the trigonal field. No specification of the nature of the $^4T_{2u}$ state was necessary, since the calculations depended only on the symmetry properties of the states involved. Either a charge-transfer excited state or one derived from the d^2p^1 configuration of Cr(III) would suffice.

The electric dipole matrix elements were then derived from those of the $^4A_{2g} \rightarrow {}^4T_{2u}$ transition, expressed by means of vector-coupling coefficients multiplied by the reduced matrix element $\langle ^4A_{2g}||\mathbf{M}||^4T_{2u}\rangle$. All $^4A_{2g} \rightarrow \Gamma$ electric dipole matrix elements could then be determined from the mixing of the state Γ with the $^4T_{2u}$ state under the effects of spin–orbit coupling and the trigonal field. This approach was conceptually similar to that of Kaizaki et al.,[22] but the parameterization of the trigonal field in terms of several reduced matrix elements between states led to a wider range of possibilities and some conclusions at odds with the earlier treatment. In particular, the net rotatory strengths for the $^4A_{2g} \rightarrow {}^2E_g$ and $^4A_{2g} \rightarrow {}^2T_{1g}$ transitions were predicted *not* to be tied directly in sign and relative magnitude to the net rotatory strength of the $^4A_{2g} \rightarrow {}^4T_{2g}$ transition. They also predicted, contrary to commonly held ideas,[24] that the sign of the net rotatory strength of the $^4A_{2g} \rightarrow {}^4T_{2g}$ transition would most often be that of the nondegenerate component, $^4A_2 \rightarrow {}^4A_1$ (D_3), rather than that of the oppositely signed degenerate component, $^4A_2 \rightarrow {}^4E$.

In 1981 Geiser and Güdel published a low-temperature single-crystal CD spectrum of $[Cr(en)_3]^{3+}$ in a host matrix.[25] In principle, the high resolution achieved permits the assignment of all five components of the $^4A_{2g} \rightarrow \{^2E_g, ^2T_{1g}\}$ transitions. This task was quite difficult, however, because of the very considerable amount of vibronic structure in the CD spectrum, as is also true of the absorption spectrum.[26] The most remarkable difference between the single-crystal and the solution spectra is that virtually all of the spin-forbidden $^4A_{2g} \rightarrow \{^2E_g, ^2T_{1g}\}$ CD peaks in the single-crystal spectrum have the same sign.

The biggest physical difference between the two experiments is that the orientation of the single crystals was such that light was propagated along the $z(C_3)$ axis. The resulting axial CD spectrum contained no contribution from magnetic or electric transition dipoles oriented in the z direction. It is also possible that significant geometrical differences at the Cr site exist between the crystal and the solution environments.

Geiser and Güdel, using an analytic approach similar to that of Kaizaki et al.,[22] concluded that the net axial rotatory strength of the $^4A_{2g} \rightarrow {}^2E_g$ and $^4A_{2g} \rightarrow {}^2T_{1g}$ transitions should have the same sign as the $^4A_2 \rightarrow {}^4E$ component of the first spin-allowed transition. They also disagreed with the previous assignment of the three peaks in the spin-forbidden region of the solution spectrum to the trigonal components of $^4A_{2g} \rightarrow \{^2E_g, ^2T_{1g}\}$, attributing at least the highest energy peak to vibronic satellites of the ^2E_g state. This argument was based in part on relative intensities expected from the model they put forward. Their own assignment of the $^2T_{1g}$ components, based on an analysis of the entire vibronic spectrum, was to three not particularly intense peaks at 15 423, 15 441, and 15 508 cm^{-1}. The overall splitting of 85 cm^{-1} is considerably smaller than the 300 cm^{-1} suggested by Kaizaki and by Richardson, which seemed too large, considering the modest 19-cm^{-1} splitting of the ^2E_g state by spin–orbit coupling and the trigonal field. The 300-cm^{-1} $^2T_{1g}$ splitting also appears to be too large because of indications from polarized CD spectra of the spin-allowed bands that the splitting of the quartets by the trigonal field (which ought to be larger than the splitting of the $^2T_{1g}$ state) amounted to no more than 100–200 cm^{-1}.[27,28]

Kaizaki et al., following a series of papers examining the spin-forbidden CD spectra of other chromium(III) complexes,[29-32] returned to $[Cr(en)_3]^{3+}$ and a series of related compounds, concluding again that the three peaks seen in the solution spectrum represent electronic transitions to the trigonal components of the ^2E_g and $^2T_{1g}$ states.[33] Using the same model as previously,[22] based on borrowing dipole strength from the nearest quartet, and using more recent experimental data on the rotational strengths of the two quartet components,[28] the predicted signs and the relative rotational strengths of the three electronic transitions were in good agreement with those seen in the solution spectrum. In addition, by adding and subtracting experimental CD spectra of pairs of diastereomers, Kaizaki was able to obtain spectra representing separately the configurational and the vicinal contributions to the rotational strengths. The vicinal CD spectra show a splitting of the $^4A_{2g} \rightarrow {}^2E_g$ transition into two narrow components of opposite sign. Although the observed splittings of ca. 100 cm^{-1} seem too large, compared to the 19-cm^{-1} splitting seen in crystals,[25,26] the effect already noted, by which CD peaks of opposite sign cancel in the area between the actual component extrema and appear to move the peak positions to the wings, is reinforced by the large bandwidths in the room-temperature spectra. Again no explanation of the 300-cm^{-1} trigonal splitting of the $^2T_{1g}$ state was offered.

Recently we have shown that the geometric distortions that tris(bidentate) complexes are subject to can lead to large splittings of the $^2T_{1g}$ state while ^2E_g splittings remain small.[34] The AOM derivation of the ligand field potential in this treatment can also be applied to calculations of rotatory strengths, and geometric

(19) Kling, O.; Woldbye, F. *Acta Chem. Scand.* **1961**, *15*, 704.
(20) McCaffery, A. J.; Mason, S. F. *Trans. Faraday Soc.* **1963**, *59*, 1.
(21) Kaizaki, S.; Hidaka, J.; Shimura, Y. *Bull. Chem. Soc. Jpn.* **1970**, *43*, 1100.
(22) Kaizaki, S.; Hidaka, J.; Shimura, Y. *Inorg. Chem.* **1973**, *12*, 142.
(23) Hilmes, G. L.; Brittain, H. G.; Richardson, F. S. *Inorg. Chem.* **1977**, *16*, 528.
(24) Mason, S. F. In *Fundamental Aspects and Recent Developments in Optical Rotatory Dispersion and Circular Dichroism*; Ciardelli, F., Salvadori, P., Eds.; Heyden: London, 1973, Chapter 3.6.
(25) Geiser, U.; Güdel, H. U. *Inorg. Chem.* **1981**, *20*, 3013.
(26) Flint, C. D.; Matthews, A. P. *J. Chem. Soc., Faraday Trans. 2* **1976**, *72*, 579.
(27) Jensen, H. P. *Appl. Spectrosc.* **1980**, *34*, 360.
(28) Jensen, H. P. *Acta Chem. Scand. Ser. A* **1980**, *A34*, 355.
(29) Kaizaki, S.; Shimura, Y. *Bull. Chem. Soc. Jpn.* **1975**, *48*, 3611.
(30) Kaizaki, S.; Mori, H. *Chem. Lett.* **1981**, 567.
(31) Kaizaki, S.; Ito, M. *Bull. Chem. Soc. Jpn.* **1981**, *54*, 2499.
(32) Kaizaki, S.; Mori, H. *Bull. Chem. Soc. Jpn.* **1981**, *54*, 3562.
(33) Kaizaki, S.; Ito, M.; Nishimura, N.; Matsushita, Y. *Inorg. Chem.* **1985**, *24*, 2080.
(34) Hoggard, P. E. *Coord. Chem. Rev.* **1986**, *70*, 85.

Table II. Elements of the Transformation Matrix **D**, Which Rotates the p and d Orbitals To Point in the Direction (θ, ϕ)

orbital	$\mathbf{D}^{\sigma}$	$\mathbf{D}^{\pi c}$	$\mathbf{D}^{\pi s}$
p_x	$\sin\theta\cos\phi$	$\cos\theta\cos\phi$	$-\sin\phi$
p_y	$\sin\theta\sin\phi$	$\cos\theta\sin\phi$	$\cos\phi$
p_z	$\cos\theta$	$-\sin\theta$	0
d_{xy}	$(\sqrt{3}/4)(1-\cos 2\theta)\sin 2\phi$	$(1/2)\sin 2\theta\sin 2\phi$	$\sin\theta\cos 2\phi$
d_{xz}	$(\sqrt{3}/2)\sin 2\theta\cos\phi$	$\cos 2\theta\cos\phi$	$-\cos\theta\sin\phi$
d_{yz}	$(\sqrt{3}/2)\sin 2\theta\sin\phi$	$\cos 2\theta\sin\phi$	$\cos\theta\cos\phi$
$d_{x^2-y^2}$	$(\sqrt{3}/4)(1-\cos 2\theta)\cos 2\phi$	$(1/2)\sin 2\theta\cos 2\phi$	$-\sin\theta\sin 2\phi$
d_{z^2}	$(1/4)(1+3\cos 2\theta)$	$(-\sqrt{3}/2)\sin 2\theta$	0

effects of the ligands and other atoms in the molecule on the dissymmetry can be explicitly included. Orbital eigenfunctions are obtained directly from the diagonalization procedure, and are linear combinations of all 120 three-electron basis functions from the d^3 configuration. It is therefore appropriate to reexamine the issues related to $[Cr(en)_3]^{3+}$: the relative rotational strengths of the spin-forbidden bands, the assignment of the $\{^2E_g, {}^2T_{1g}\}$ components, the magnitude of the trigonal splitting of the $^2T_{1g}$ state, and whether or not the axial CD spectrum of the crystal should differ so markedly from the spectrum of the solution.

Theory and Calculations

Methods to determine the eigenvalues and eigenfunctions of a d^3 ion in a ligand field of any geometry have been described elsewhere.[34] We use the full set of 120 single-term antisymmetrized product wave functions as a basis. The Hamiltonian function

$$\mathcal{H} = \sum_{i<j}\frac{e^2}{r_{ij}} + V_{LF} + \xi\sum_i \mathbf{l}_i\cdot\mathbf{s}_i + \alpha_T\sum_i \mathbf{l}_i^2 + 2\alpha_T\sum_{i<j}\mathbf{l}_i\cdot\mathbf{l}_j \quad (6)$$

includes interelectronic repulsion, spin–orbit coupling, a Trees correction[35] in the form of orbit–orbit repulsion, and a ligand field potential expressed in the AOM formalism as a summation of σ- and π-interactions from each ligand.[36] The eigenfunctions are obtained after optimization to fit the eigenvalues to experimental absorption or excitation spectra, particularly of the sharp intraconfigurational transitions, which give rise to single, distinguishable bands in correspondence with particular eigenfunctions.

Electric Dipole Matrix Elements. As in several previous expositions, we assume that nonzero electric dipole moments can be attributed to the mixing of p character into the d orbitals under the static, equilibrium molecular symmetry. The angular overlap model provides a straightforward means to evaluate this mixing.

The AOM ligand potential is constructed by rotating the coordinate system for one ligand at a time so that the d_{z^2} orbital points directly at the ligand. The interaction of the ligand L with the metal now raises the energy of the rotated d_{z^2} orbital by $e_{\sigma L}$ and alters the energies of the d_{xz} and d_{yz} orbitals by $e_{\pi cL}$ and $e_{\pi sL}$, respectively (c and s refer to the cosine and sine dependence of xz and yz on the azimuthal angle ϕ). Rotating the coordinate system back again spreads these effects through the original set of d orbitals. The process is repeated for all ligands.

Inclusion of the p orbitals in the transformation matrix allows the ligand effects on these orbitals to be evaluated at the same time. Table II illustrates the transformation matrix for the special case of isotropic ligands, i.e., ligands whose π-interaction with the metal is the same regardless of orientation. Then $e_{\pi c} = e_{\pi s}$, and the angular coordinates (θ, ϕ) of the ligand are sufficient to specify the coordinate transformation. In the general case a third angle, ψ, is required to fix the orientation of the new xy plane. The full transformation matrices are given by Schäffer.[36]

Table II contains the complete matrix to rotate the z axis to point in the direction (θ, ϕ) and express the new p orbitals as linear combinations of the old ones. It contains only part of the matrix for the d orbitals, since we are not concerned with the new d_{xy} and $d_{x^2-y^2}$ orbitals, which could only δ bond with the ligand. With $\mathbf{D}^{-1} = \mathbf{D}^T$ used to accomplish the back-transformation, the ligand potential is then expressed for a general matrix element between orbitals d_i and d_j as[36]

$$\langle d_i|V|d_j\rangle = \sum_{L=1}^{N}[D_i^{\sigma L}D_j^{\sigma L}e_{\sigma L} + D_i^{\pi sL}D_j^{\pi sL}e_{\pi sL} + D_i^{\pi cL}D_j^{\pi cL}e_{\pi cL}] \quad (7)$$

where the sum is over all N ligands, each represented by AOM parameters $e_{\sigma L}$, $e_{\pi sL}$, and $e_{\pi cL}$ (the latter two will be equal for isotropically bonding ligands). D_i and D_j represent the **D** matrix entries from the rows labeled d_i and d_j. In effect, eq 7 represents the mixing of the d orbitals caused by the presence of the ligands in any number or geometric relationship.

We may also evaluate the mixing of the p orbitals under the ligand field

$$\langle p_i|V|p_j\rangle = \sum_{L=1}^{N}[D_{i'}^{\sigma L}D_{j'}^{\sigma L}e_{p\sigma L} + D_{i'}^{\pi sL}D_{j'}^{\pi sL}e_{p\pi sL} + D_{i'}^{\pi cL}D_{j'}^{\pi cL}e_{p\pi cL}] \quad (8)$$

where this time $D_{i'}$ and $D_{j'}$ refer to **D** elements in the rows labeled p_i and p_j. The AOM parameters $e_{p\sigma}$, $e_{p\pi c}$, and $e_{p\pi s}$ represent the amounts by which the p_z, p_x, and p_y orbitals are increased in energy by a ligand located on the z axis. These will not be equal to e_σ, $e_{\pi c}$, and $e_{\pi s}$ defined over the d orbitals, but it is reasonable to assume that they are related by a common factor, so that for all ligands L

$$\begin{aligned} e_{p\sigma L} &= f_\sigma e_{\sigma L} \\ e_{p\pi cL} &= f_\pi e_{\pi cL} \\ e_{p\pi sL} &= f_\pi e_{\pi sL} \end{aligned} \quad (9)$$

In the same manner we can generate the terms of the off-diagonal $\langle p_i|V|d_j\rangle$ block, which determine the extent of p–d mixing under the ligand field.

$$\langle p_i|V|d_j\rangle = \sum_{L=1}^{N}[D_{i'}^{\sigma L}D_j^{\sigma L}\epsilon_{p\sigma L} + D_{i'}^{\pi sL}D_j^{\pi sL}\epsilon_{p\pi sL} + D_{i'}^{\pi cL}D_j^{\pi cL}\epsilon_{p\pi cL}] \quad (10)$$

Again $D_{i'}$ refers to the row of **D** corresponding to the p_i orbitals, and D_j to the **D** elements in the d_j row, and ϵ_σ and ϵ_π represent the extent of p–d mixing via metal–ligand σ- and π-interactions in the local C_{2v} M–L environment. We can reasonably assume that these are proportional to the d-orbital e_σ and e_π AOM parameters, and we assume also that the proportionality constant is the same for σ and π.

$$\begin{aligned} \epsilon_{\sigma L} &= g e_{\sigma L} \\ \epsilon_{\pi cL} &= g e_{\pi cL} \\ \epsilon_{\pi sL} &= g e_{\pi sL} \end{aligned} \quad (11)$$

The **D** matrix for each ligand is determined from the angular coordinates of the ligand, while the e_σ and e_π parameters are arrived at through the energy optimization, that is, through a spectral fitting process. As an example, a $\langle p|V|d\rangle$ matrix has been calculated for a regular Λ-$[Cr(en)_3]^{3+}$ complex with D_3 symmetry and is shown in Table III. The positions of the nitrogen atoms used to generate the matrix are those resulting from Cartesian bite and twist angles of 4.0 and +1.0°, respectively. The Cartesian bite angle α is the angular displacement of a coordinated atom from a Cartesian axis. The Cartesian twist angle β is the displacement of an N–N pair above and below a Cartesian plane.[34] AOM parameters $e_\sigma = 7000\ cm^{-1}$ and $e_\pi = 0$ were used. The

Table III. $\langle p|V|d\rangle$ Matrix Calculated for $[Cr(en)_3]^{3+}$ [a]

	d_{xy}	d_{xz}	d_{yz}	$d_{x^2-y^2}$	d_{z^2}
p_x	−967	967	0	−484	−837
p_y	967	0	−967	−484	837
p_z	0	−967	967	967	0

[a] $e_\sigma = 7000\ cm^{-1}$, $e_\pi = 0\ cm^{-1}$, $\alpha = 4.0°$, $\beta = +1.0°$. Values in cm^{-1}.

(35) Trees, R. E. *Phys. Rev.* **1951**, *83*, 756.
(36) Schäffer, C. E. *Struct. Bonding (Berlin)* **1968**, *5*, 68.

Table IV. Matrix Elements $\langle p|\mathbf{r}|d\rangle$ of the Electric Dipole Operator

	d_{xy}	d_{xz}	d_{yz}	$d_{x^2-y^2}$	d_{z^2}
p_x	$\sqrt{3}i\mathbf{i}$	0	$\sqrt{3}i\mathbf{k}$	$-\sqrt{3}i\mathbf{j}$	$-i\mathbf{j}$
p_y	$\sqrt{3}i\mathbf{j}$	$\sqrt{3}\mathbf{i}$	$\sqrt{3}\mathbf{j}$	$\sqrt{3}i\mathbf{i}$	$-i\mathbf{i}$
p_z	0	$-\sqrt{3}\mathbf{i}$	0	0	$2\mathbf{k}$

unknown proportionality factor g is not included, so the units in Table III are essentially arbitrary.

This $\langle p|V|d\rangle$ matrix is equivalent to one generated from symmetry considerations alone, using the spherical harmonic term $(Y_3^3 - Y_3^{-3})$ as the perturbing term. Those presented in earlier treatments differ only in that they use a trigonally quantized basis set with the (1, 1, 1) C_3 axis as the z axis, whereas our z axis is tetragonally quantized and for Table III is chosen to align two nitrogens at opposite ends with the minimum possible displacements from the axis. However, we are not bound to D_3 symmetry. The $\langle p|V|d\rangle$ matrix can be generated for any set of ligand positions or whatever other atoms are creating the dissymmetric potential at the metal center. Furthermore, the ligands need not be restricted to isotropic bonding. Anisotropic π-interaction by coordinating atoms arrayed in D_3 symmetry can lead to a far less symmetric perturbation of the metal environment.

The $\langle p|\mathbf{r}|d\rangle$ matrix elements[37] of the electric dipole operator are listed in Table IV for the basis set of real p and d orbitals we are employing. A first-order perturbation of the d orbitals by the ligand field yields for the electric dipole matrix elements between the d orbitals

$$\langle d_i|\mathbf{Q}|d_j\rangle = -\sum_k \frac{\langle d_i|\mathbf{Q}|p_k\rangle\langle p_k|V|d_j\rangle}{E(p_k) - E(d_j)} - \sum_k \frac{\langle d_i|V|p_k\rangle\langle p_k|\mathbf{Q}|d_j\rangle}{E(p_k) - E(d_i)} \tag{12}$$

We assume, for computational purposes, that the energies of the three p orbitals are identical. The one-electron d orbital energies, $E(d_i)$, may be approximated by neglecting spin–orbit coupling, as the diagonal elements of the ligand field potential, $\langle d_i|V|d_i\rangle$. There is little advantage to refining the denominators in eq 12, since the d–p energy gap should be sizable. The expression used to compute the electric dipole matrix element is then

$$\langle d_i|\mathbf{Q}|d_j\rangle = -\sum_k \left[\frac{\langle d_i|\mathbf{Q}|p_k\rangle\langle p_k|V|d_j\rangle}{E_p - \langle d_j|V|d_j\rangle} + \frac{\langle d_i|V|p_k\rangle\langle p_k|\mathbf{Q}|d_j\rangle}{E_p - \langle d_i|V|d_i\rangle} \right] \tag{13}$$

The $\langle d|V|d\rangle$ matrix elements are evaluated as discussed elsewhere.[34] The p orbital energy, E_p, is unknown. It can be left as a parameter in the fitting process, but the relative rotational strengths are not particularly sensitive to the value used, so we have chosen to keep E_p fixed at 75 000 cm^{-1}. The one-electron matrix elements $\langle d_i|\mathbf{Q}|d_j\rangle$ from eq 13 are then used to set up the 120 × 120 **Q** matrix between three-electron functions, $\langle\phi_i|\mathbf{Q}|\phi_j\rangle$.

Magnetic Dipole Matrix Elements. The matrix elements of **l** and **s** are readily evaluated over the spherical harmonic d orbital basis, so that eq 3 can be used to calculate the magnetic dipole matrix elements. After being transformed to the real d basis with spin, the one-electron matrix elements of $\mathbf{l} + 2\mathbf{s}$ are as shown in Table V. These are then converted to the 120 × 120 matrix $\langle\phi_i|\mathbf{M}|\phi_j\rangle$ in the basis of real three-electron functions.

Rotational Strengths. To evaluate rotational strengths for d^3 complexes the 120 × 120 secular determinant is diagonalized and the eigenfunctions determined.[34] Rotational strengths are then calculated from eq 2. For odd-electron systems all the eigenfunctions will occur in Kramers-degenerate pairs. The $^4A_{2g}$ ground state (in O_h notation) consists of two such pairs, usually split by less than 2 cm^{-1} by the ligand field. Thus all four eigenfunctions contribute to the rotational strength of all electronic transitions, even relatively narrow ones. Any dissymmetric complex has a symmetry such that with spin–orbit coupling there are no degeneracies outside of Kramers degeneracy. The components of the $^4T_{2g}$ and $^4T_{1g}$ states, however, cannot be sufficiently resolved to distinguish six components experimentally. This is particularly true for tris(bidentate) complexes, for which the splittings are usually quite small.

There are, however, eight Kramers doublet excited states derived from the O_h t_{2g}^3 configuration, transitions to which are generally narrow in absorption or CD spectra. Even one of these "single-component" transitions consists of eight nearly degenerate (except for the ground-state splitting) subcomponents, the rotational strengths of which must be summed to yield the total for the observed band. At low temperatures these components can often be easily distinguished in absorption or CD spectra, but at room temperature the bandwidths may exceed the splittings. These transitions are all spin-forbidden and very weak. In the present model the inclusion of spin–orbit coupling is critical, because otherwise all the electric dipole matrix elements between states of different spin multiplicities would be zero.

If we continue with our example of Λ-$[Cr(en)_3]^{3+}$ in an idealized D_3 geometry, with a Cartesian bite angle of 4.0° and a Cartesian twist angle of +1.0°, using suitable (but not optimized) parameters, Table VI shows the calculated rotational strengths for the lowest energy electronic transition, from the $^4A_{2g}$ to one component of ^2E_g. In Table VI the rotatory strengths are normalized to a value of 1.00 for the strongest subcomponent. The total rotatory strength for the transition is +3.33 on this scale. The splitting of the ground state is calculated to be 0.2 cm^{-1}, with separate rotatory strengths of 2.17 and 1.16 for the two components. These would not be distinguishable in a CD spectrum, even at very low temperatures.

From the calculated rotatory strengths for components of other electronic transitions, it can be seen that there is no general relationship between the signs or magnitudes of transitions from or to two members of a Kramers doublet. Nor are the two distinct ground-state components related in sign or magnitude. In subsequent discussion we will refer to the net rotatory strength of such a grouping of eight constituent transitions as belonging to a single component. Normally the two parts of this component, arising from the ground-state splitting, will be spectroscopically indistinguishable. When the signs are opposite, however, a narrow CD peak might show some vestige of ground-state splitting.

In this model there are two ways in which the geometry affects rotatory strengths. One is through p–d mixing. For the Λ-$[Cr(en)_3]^{3+}$ example one may consider this to be determined by the D_3 point group symmetry alone. No change in the Cartesian bite or twist angles affects the relative values of the $\langle p|V|d\rangle$ matrix elements. Except for the absolute magnitude, the rotational strengths of all transitions are unaffected by geometric changes that preserve D_3 symmetry. A distortion that destroys a symmetry axis, however, produces changes in the relative values of $\langle p|V|d\rangle$ matrix elements that depend on the extent of the distortion. The p–d mixing caused by anisotropic ligand to metal π-bonding falls in this category as well.

The second point of geometric influence is in the eigenfunctions, through the ligand field potential. Through alterations in the eigenfunctions, symmetry-preserving distortions do affect the relative rotational strengths of different transitions. This analysis of the consequences of geometric changes is approximately equivalent to Richardson's partitioning of the static perturbation into ungerade and gerade terms.[12]

Conformational and Vicinal Effects. The model provides a direct means to account for conformational and vicinal effects on the rotational strength from the presence of noncoordinated atoms. The angular positions of these atoms can be used to generate additive contributions to the $\langle p|V|d\rangle$ matrix, used to generate the electric dipole perturbation, and to the $\langle d|V|d\rangle$ matrix, from which the eigenfunctions and transition energies are derived. Contributions to the ligand potential from atoms more distant than those in the first coordination sphere are probably best represented in terms of σ-bonding only, through an AOM e_σ parameter.[38] Even

(37) Slater, J. C. *Quantum Theory of Atomic Structure*; McGraw-Hill: New York, 1960, Vol. II, Chapter 25.

(38) Hoggard, P. E.; Lee, K.-W. *Inorg. Chem.* **1988**, *27*, 2335.

Table V. Matrix Elements $\langle d_i|L + 2S|d_j\rangle$ of the Magnetic Dipole Operator

	$(xy)^+$	$(xz)^+$	$(yz)^+$	$(x^2-y^2)^+$	$(z^2)^+$	$(xy)^-$	$(xz)^-$	$(yz)^-$	$(x^2-y^2)^-$	$(z^2)^-$
$(xy)^+$	**k**	$-i$**i**	i**j**	$2i$**k**	0	**i** $-$ i**j**	0	0	0	0
$(xz)^+$		**k**	$-i$**k**	$-i$**j**	$\sqrt{3}i$**j**	0	**i** $-$ i**j**	0	0	0
$(yz)^+$			**k**	$-i$**i**	$-\sqrt{3}i$**i**	0	0	**i** $-$ i**j**	0	0
$(x^2-y^2)^+$				**k**	0	0	0	0	**i** $-$ i**j**	0
$(z^2)^+$					**k**	0	0	0	0	**i** $-$ i**j**
$(xy)^-$						$-$**k**	$-i$**i**	$-i$**j**	$2i$**k**	0
$(xz)^-$							$-$**k**	$-i$**k**	$-i$**j**	$\sqrt{3}i$**j**
$(yz)^-$								$-$**k**	$-i$**i**	$-\sqrt{3}i$**i**
$(x^2-y^2)^-$									$-$**k**	0
$(z^2)^-$										$-$**k**

Table VI. Calculated Rotatory Strengths for the Lowest Energy Electronic Transition in $[Cr(en)_3]^{3+}$ [a]

	ϕ_5	ϕ_6
ϕ_1	0.89	0.49
ϕ_2	0.20	0.59
ϕ_3	−0.37	1.00
ϕ_4	−0.42	0.95

[a] $e_{\sigma N}$ = 7000, $e_{\pi N}$ = 0, B = 650, C = 3400, ζ = 150, α_T (Trees parameter) = 0, E_p = 75000 (all in cm^{-1}). Geometry: α = 4.0°, β = +1.0°. Transition is from $^4A_{2g}(\phi_1-\phi_4)$ to one component of $^2E_g(\phi_5, \phi_6)$. Values are normalized to 1 for the largest component rotatory strength.

the sign of e_σ for saturated carbon atoms is unknown, and its value may be left to vary during the optimization.

Results and Discussion

Spin-Forbidden Single-Crystal CD Spectrum. Geiser and Güdel's low-temperature high-resolution CD spectrum of Λ-$[Cr(en)_3]^{3+}$ in a host matrix[25] differs markedly from the room-temperature solution spectrum reported by Richardson[23] and by Kaizaki.[22,33] The solution spectrum exhibits three peaks in the ^2E_g, $^2T_{1g}$ region, with positive, negative, and positive $\Delta\epsilon$. The solid-state spectrum contains a great deal of vibrational fine structure, and $\Delta\epsilon$ is positive for nearly every peak. The electronic assignments also appear to be at odds. The two higher energy peaks in the solution spectrum, split by about 300 cm^{-1}, were assigned to the $^2A_1$ and ^2E components of the $^2T_{1g}$ band.[22,23,33] Güdel, however, assigned the three components of the $^4A_{2g} \rightarrow {}^2T_{1g}$ transition with a total separation of just 84 cm^{-1} in the single-crystal spectrum.

AOM calculations do predict that the splitting of the $^2T_{1g}$ band should increase as the Cartesian bite angle increases and that this splitting is reinforced for a Λ-isomer by a negative Cartesian twist angle (meaning that, looking from the outside toward the two teeth of a chelating ligand, the coordinated atom on the right lies above a plane containing two coordinate axes, while the atom on the left lies below the same plane), and is reduced by a positive Cartesian twist angle.[34] The reverse is true for a Δ-isomer.

Given the proper distortion, the $^2T_{1g}$ splitting could amount to 300 cm^{-1} or more. At a Cartesian twist angle of 0°, the Cartesian bite angle required is about 3.5°.[34] The geometry of $[Cr(en)_3]^{3+}$ doped into a host is, of course, uncertain. We have used one site from the crystal structure of Δ-$[Cr(en)_3]Cl_3$ as a reference.[39] After inversion of the coordinates to model the Λ-isomer, the average Cartesian bite and twist angles are found to be 4.1 and 1.8°. Thus the bite and twist distortions offset each other to some extent. In addition there are significant deviations from D_3 symmetry in the $[Cr(en)_3]Cl_3$ structure.

The ligand field potential matrix, including the $\langle p|V|d\rangle$ portion used to generate the electric dipole transition matrix, was set up to include the six nitrogens at their exact positions relative to Cr, each weighted at $e_{\sigma N}$, and the six attached carbons at their exact positions (in $[Cr(en)_3]Cl_3$), with weights of $ve_{\sigma N}$. The parameter v was allowed to vary and was expected to be considerably smaller than one because the carbon atoms are further from the chromium than the nitrogens and because they cannot donate electron density through lone pairs. In fact it is unclear whether v should be positive or negative. The contribution of the carbon atoms to the electric dipole transition matrix can, however, be important, the more so as the nitrogen atoms approach a distortion-free octahedral arrangement.

It has been demonstrated that the field generated by the counterions also affects energy levels and splittings significantly[38,40] and can be presumed to affect the rotational strengths as well, through the electric dipole transition matrix. The host matrix used by Geiser and Güdel was Δ-2$[Ir(en)_3]Cl_3 \cdot KCl \cdot 6H_2O$, for which there are no crystallographic data. We attempted to take some account of the influence of the anion field by including the nearest 14 Cl^- ions from the structure of Δ-$[Cr(en)_3]Cl_3$ in the ligand field potential. However, the effects on the calculated transition energies and splittings were very small, most probably because the geometry of 12 of the anions corresponds approximately to the edges of a cube centered on the coordination octahedron, thus providing only a very small nonoctahedral perturbation. The anion field has therefore been ignored in the calculations reported here.

An optimization was undertaken to fit the data of Geiser and Güdel as assigned by them.[25] The variable parameters were $e_{\sigma N}$, the interelectronic repulsion parameters B, C, and α_T, the spin–orbit coupling parameter ζ, and the coefficient v measuring the contribution of the carbon atoms to the total ligand field potential relative to the nitrogen atoms. Geiser and Güdel worked with an oriented crystal, with light passing through a face in a direction parallel to the trigonal crystal axis (assumed to be colinear with the molecular C_3 axes). The rotatory strengths thereby observed are axial rotatory strengths, with only two degrees of freedom for electric and magnetic dipole transitions. Equation 2 thus becomes

$$R(0\rightarrow j) = \mathrm{Im}[\langle\psi_0|Q_x|\psi_j\rangle\langle\psi_j|M_x|\psi_0\rangle + \langle\psi_0|Q_y|\psi_j\rangle\langle\psi_j|M_y|\psi_0\rangle] \quad (14)$$

The coordinates of the six nitrogens and six carbons were transformed so that the z axis was the direction of propagation. A least-squares optimization was performed on the energies of the five $^4A_{2g} \rightarrow ({}^2E_g, {}^2T_{1g})$ transitions and the average energies (over the six spin–orbit components) of the $^4A_{2g} \rightarrow {}^4T_{2g}$ and $^4A_{2g} \rightarrow {}^4T_{1g}$ transitions. Geiser and Güdel did not report $\bar{\nu}_{max}$ for the spin-allowed transitions. We have used values from the room-temperature solution spectrum,[33] which agree satisfactorily with the spectrum presented in Güdel's paper.

The function minimized was

$$f = \sum(\Delta E_Q)^2 + 10^2\sum(\Delta E_D)^2 + 10^4(\Delta S)^2 \quad (15)$$

where ΔE_Q, ΔE_D, and ΔS represent differences between experimental and calculated quartet and doublet transition energies, and the splitting of the ^2E_g state, respectively. The resulting fit, shown in Table VII, is satisfactory, especially considering the approximations to the geometry of the complex. When optimi-

(39) Whuler, A.; Brouty, C.; Spinat, P.; Herpin, P. *Acta Crystallogr., Sect. B: Struct. Crystallogr. Cryst. Chem.* **1977**, *B33*, 2877.

(40) Hoggard, P. E.; Lee, K.-W. In *Photochemistry and Photophysics of Coordination Compounds*; Yersin, H., Vogler, A., Eds.; Springer-Verlag: West Berlin, 1987; p 49.

Table VII. Observed and Calculated Transition Energies and Relative Rotational Strengths for Λ-$[Cr(en)_3]Cl_3$[a]

transition (D_3 notation)	ΔE, cm^{-1}		$\Delta\epsilon$[b]	
	obsd[c]	calcd[d]	obsd[c]	calcd[d]
$^4A_2 \rightarrow {}^2E_a$ (^2E_g)	14881	14884	+1.00	+1.00
$\rightarrow {}^2E_b$ (^2E_g)	14900	14903	+0.95	+0.36
$\rightarrow {}^2A_1$ ($^2T_{1g}$)	15423	15424	+0.36	+0.04
$\rightarrow {}^2E_a$ ($^2T_{1g}$)	15441	15450	+0.50	+0.16
$\rightarrow {}^2E_b$ ($^2T_{1g}$)	15507	15492	−0.23	+0.31
$\rightarrow {}^4A_2$, ^4E ($^4T_{2g}$)	22350	22180	1200	1820
$\rightarrow {}^4A_1$, ^4E ($^4T_{1g}$)	28670	28780		

[a] Measurements at T = 8 K in a $2[Ir(en)_3]Cl_3 \cdot KCl \cdot 6H_2O$ host. Calculations for $[Cr(en)_3]Cl_3$. [b] Relative to $\Delta\epsilon(^4A_{2g} \rightarrow {}^2E_g) = 1.00$. [c] References 25 and 33. [d] Best-fit parameters (in cm^{-1}, except for v): $e_{\sigma N} = 7591 \pm 107$, $B = 682 \pm 7$, $C = 2984 \pm 93$, $\alpha_T = 117 \pm 37$, $\zeta = 274 \pm 50$, $v = -0.0834 \pm 0.018$.

zations to alternative assignments were attempted, in particular assignments in which the total $^2T_{1g}$ splitting was near 300 cm^{-1}, the fit was very much worse. The error limits on the parameters in Table VII were determined by the propagation of estimated experimental uncertainties, as described elsewhere.[34]

Following optimization, rotational strengths were calculated with eq 14, and the results are included in Table VII. The signs are in agreement with observation, except that $\Delta\epsilon$ of the fifth doublet was calculated to be positive, whereas Geiser and Güdel had assigned it to a small negative CD peak, one of the very few in the spectrum. The relative magnitudes match those from experiment only moderately well. However, even this degree of agreement is quite encouraging, since all the parameters and eigenfunctions used in the calculation of the rotational strengths were taken from the transition energy optimization. No additional adjustable parameters were were introduced, nor were the rotational strengths taken into account during the optimization.

In fact, including the rotational strength data in the function minimized during optimization (eq 15) did not appreciably alter the results shown in Table VII. Neither did assigning a zero weight to the transition energy of the fifth doublet. Except for the sign of $\Delta\epsilon$ of that fifth peak, these calculations lend strong confirmation to the assignments proposed by Geiser and Güdel.

The parameters from the best-fit solution shown in Table VII generally fall within the normal bounds for each. Two deserve comment. The Trees parameter, $\alpha_T = 117$ cm^{-1}, appears high compared to the commonly quoted free-ion value of 70 cm^{-1} for Cr(III).[4] But systems in which α_T has been allowed to vary have led to uniformly higher values, often as high as 200 cm^{-1}.[34,38,41] The parameter v optimized at −0.0834, corresponding to an effective e_σ for carbon of −633 cm^{-1}, implying a stabilization of the chromium d orbitals by interaction with the carbons. This may be attributable to the field from the residual nuclear charge from the carbon atoms. The spin–orbit coupling parameter, $\zeta = 274$ cm^{-1}, was in the range of a penalty function designed to restrain it from exceeding the value in the free ion (275 cm^{-1}).[4]

Spin-Forbidden Solution CD Spectrum. Similar calculations were undertaken to model $[Cr(en)_3]^{3+}$ in solution. The $\langle d_i|V|d_j\rangle$ matrix from the ligand field potential of the six nitrogens was calculated as a function of the Cartesian bite and twist angles as described in the previous section. The effects of the carbon atoms on the rotational strengths can be treated if we assume that the individual carbon rings will adopt one of the two most stable conformations, commonly referred to as *lel* and *ob*. If the conformations of all three chelate rings are identical, the molecule retains D_3 symmetry, and the carbon positions can be fully described by Cartesian bite and twist angles. From crystal structures,[42,43] we estimate α and β to be 31 and 22° for the lel_3 conformation, and 31 and −25° for the ob_3 conformation (both with reference to the Λ-enantiomer).

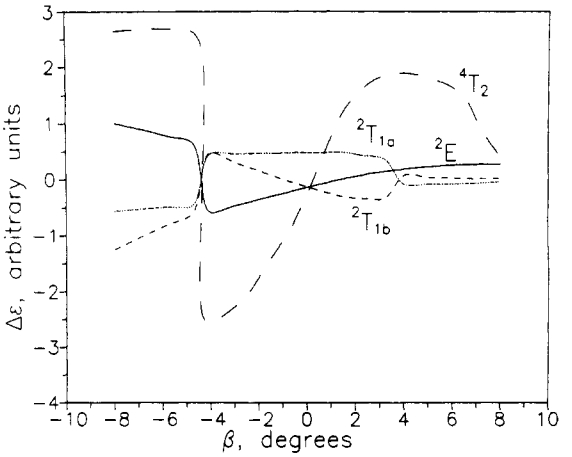

Figure 1. Calculated variation of the relative rotatory strengths, for lel_3-Λ-$[Cr(en)_3]^{3+}$ in solution, of the transitions from the $^4A_{2g}$ state to the ^2E_g (two components), $^2T_{1a}$ (one component), $^2T_{1b}$ (two components), and $^4T_{2g}$ (six components) states as a function of the Cartesian twist angle β. Other parameters: $\alpha_N = 4.1°$, $e_{\sigma N} = 7500$ cm^{-1}, $B = 700$ cm^{-1}, $C = 2850$ cm^{-1}, $\alpha_T = 170$ cm^{-1}, $\zeta = 185$ cm^{-1}, $v = -0.08$. $\Delta\epsilon$ for the $^4T_{2g}$ band is reduced by a factor of 100.

If the lel_3 conformation is assumed to be the dominant one in solution,[44,45] adding a contribution to the ligand field from the carbon atoms does not cause large changes in the relative rotational strengths, since the elements of the $\langle p|V|d\rangle$ interaction matrix remain in the same proportion for any perturbation with D_3 symmetry. The carbon atom field may, however, change the sign of the $\langle p|V|d\rangle$ matrix under certain conditions. To model the lel_3 conformation, therefore, a contribution from the carbon atoms was included with the same factor v as was found above for the crystalline state.

The criteria for a good fit to the experimental CD and excitation data are not well-defined, since the five $\{^2E_g, {}^2T_{1g}\}$ components are condensed into three observable bands. The overlapping of components of opposite sign tends to drive the observed peak positions toward the wings, obscuring the exact transition energies of the individual components. Thus the 300-cm^{-1} splitting assigned by Kaizaki[22,33] and by Richardson[23] to the $^2T_{1g}$ components could result from a $^2T_{1g}$ splitting much smaller than 300 cm^{-1}, given appropriate bandwidths.

We found it difficult, however, to model this situation satisfactorily. The two ^2E_g components were calculated to have opposite signs under almost any circumstances, so the splitting would have to be quite small in order for both peaks to appear under the same envelope, without evidence of a sign change in either wing. However with the D_3 geometry these are just the conditions leading to very small $^2T_{1g}$ splittings as well, too small to reasonably be able to generate a 300-cm^{-1} peak separation through cancellation.

An attempt to match the experimental data using the lel_3 conformation is shown in Table VIII. No attempt was made at a rigorous fit. As can be seen from Figure 1, the signs and relative magnitudes of the $\{^2E_g, {}^2T_{1g}\}$ peaks in the CD spectrum are quite sensitive to the Cartesian twist angle and taken together with the transition energies could be used to determine both α and β to within 0.5° or better, provided of course that the geometry in solution is actually lel_3. This is a significant point because with the transition energies alone it is essentially impossible to fix the values of α and β, because their effects on the sharp-line splittings are so similar.[34]

It is apparent that the calculated $^2T_{1g}$ splitting shown in Table VIII is much too small to account for the 300-cm^{-1} separation observed experimentally. With other choices for α and β, the calculated signs of the $\{^2E_g, {}^2T_{1g}\}$ CD components are not in accord

(41) Lee, K.-W.; Hoggard, P. E. *Inorg. Chem.* **1988**, *27*, 907.
(42) Whuler, A.; Brouty, C.; Spinat, P.; Herpin, P. *Acta Crystallogr., Sect. B: Struct. Crystallogr. Cryst. Chem.* **1975**, *B31*, 2069.
(43) Raymond, K. N.; Ibers, J. A. *Inorg. Chem.* **1968**, *7*, 2333.
(44) Corey, E. J.; Bailar, J. C. *J. Am. Chem. Soc.* **1959**, *81*, 2620.
(45) Niketic, S. R.; Rasmussen, K. *Acta Chem. Scand., Ser. A* **1978**, *A32*, 391.

Table VIII. Observed and Calculated Transition Energies and Relative Rotational Strengths for Λ-$[Cr(en)_3]^{3+}$ in lel_3 and lel_2ob Conformations

transition (O_h (D_3) notation)	ΔE, cm^{-1}			$\Delta\epsilon$[a]		
		calcd			calcd	
	obsd[b]	lel_3[c]	lel_2ob[d]	obsd[b]	lel_3[c]	lel_2ob[d]
$^4A_2 \rightarrow {}^2E_g$	14930	14928	14957	+1.00	+1.00	+1.00
		14941	14962		−0.82	+0.17
$\rightarrow {}^2T_{1g}$	15420	15501	15436	−0.40	−0.10	−0.08
$\rightarrow$	15720	15514	15589	+0.40	−0.09	+0.17
$\rightarrow$		15533	15602		+0.15	+0.25
$\rightarrow {}^4T_{2g}$ ($^4A_1$)	22030	21530[e]	22860[f]	+100	+4140	−2400
(^4E)		21700[g]	22970[h]		−4080	+7400
$\rightarrow {}^4T_{1g}$ (^4E)	28570	28060[i]	29380[i]			
($^4A_2$)	30680	27868	30020			

[a] Relative to $|\Delta\epsilon| = 1.0$ for the lowest energy $^4A_{2g} \rightarrow {}^2E_g$ transition. [b] Reference 33. [c] $\alpha_N = 4.30°$, $\beta_N = 4.03°$, $e_{\sigma N} = 7495\ cm^{-1}$, $B = 702\ cm^{-1}$, $C = 2843\ cm^{-1}$, $\alpha_T = 171\ cm^{-1}$, $\zeta = 185\ cm^{-1}$, $v = -0.0708$. [d] $\alpha_N = 4.10°$, $\beta_N = 1.48°$, $e_{\sigma N} = 7837\ cm^{-1}$, $B = 702\ cm^{-1}$, $C = 2946\ cm^{-1}$, $\alpha_T = 122\ cm^{-1}$, $\zeta = 155\ cm^{-1}$, $v = -0.146$. [e] 21530, 21530 cm^{-1}. [f] 22850, 22880 cm^{-1}. [g] 21620, 21700, 21720, 21760 cm^{-1}. [h] 22960, 22970, 22980, 22980 cm^{-1}. [i] $^4A_2$ and ^4E are inverted with the two choices of β_N.

with the experimental spectrum, or the ^2E_g splitting is too large, or both occur. Another possibility, of course, is that all three $^2T_{1g}$ components are found under the band envelope of the 15400-cm^{-1} peak, while the 15720-cm^{-1} peak represents one or more vibrational satellites based on the ^2E_g origins. We note that a Cartesian twist angle of approximately +4° is required in order to achieve the proper CD signs for the transition to the ^2E_g state, the lowest component of the $^2T_{1g}$ state, and the $^4T_{2g}$ states. This is about 2° more twist than in crystalline $[Cr(en)_3]Cl_3$, but does agree with Kepert's predictions for the minimum-repulsion geometry in tris(bidentate) complexes.[46]

A more likely explanation is that a lel_2ob conformation prevails in solution. Under these circumstances it is easily possible to find conditions under which large $^2T_{1g}$ splittings are calculated to occur alongside small ^2E_g splittings. The third column of Table VIII shows an approximate fit to the experimental data using carbon positions in which two rings are *lel* and one *ob*, after varying the contribution to the ligand field (and the electric dipole moment) from the carbon atoms through the parameter v discussed above to achieve an approximate best fit. Note that the Cartesian twist angle is 1.5° for the case illustrated in Table VIII, close to the average twist angle in the $[Cr(en)_3]Cl_3$ site used in the analysis of the solid-state spectrum, but somewhat smaller.

The smaller twist angle is in part responsible for the larger calculated $^2T_{1g}$ splitting than in the solid state. The other factor is the larger value of v for the calculation used to generate Table VIII (−0.146 vs 0.083 in the solid). Without knowing the actual locations of all $^4A_{2g} \rightarrow \{^2E_g, {}^2T_{1g}\}$ components, all parameter values must be regarded as very uncertain. However, a larger value of v in solution could be a result of perturbations from sources other than the carbon atoms, most likely the nearest solvation shell.

Implicit in the foregoing analysis is the assumption that the observed intensity in the sharp-line solution CD spectrum derives from the pure electronic transitions. The main justification is empirical—unambiguous assignments of sharp lines in solution spectra to vibronic transitions are rare, though by no means lacking.[29] Since the axial single-crystal spectrum is dominated by vibronic bands,[25] it is certainly possible that much of the intensity in the solution spectrum is vibronic. This may affect the proper location of the pure electronic peaks (already uncertain because of unresolved splittings) but should not affect the perceived signs of the rotational strengths, because of the tendency of vibronic peaks to mirror the signs of the electronic origins with which they are associated.[25,29]

Spin-Allowed Bands. It is widely accepted that the CD peak observed for the lowest energy $A \rightarrow T(O_h)$ transition ($d_{xy} \rightarrow d_{x^2-y^2}$ and permutations) in tris(bidentate) complexes of Cr(III) and Co(III) in solution consists of the residual rotational strength from the cancellation of oppositely signed and almost degenerate $A \rightarrow E(D_3)$ and $A \rightarrow A(D_3)$ components.[24] Our calculations support this view for $[Cr(en)_3]^{3+}$. All four spin–orbit components of the $^4A_2 \rightarrow {}^4E(D_3)$ transition were found to have rotational strengths of the same sign over the range of geometric and ligand field parameters tested, as did the two $^4A_2 \rightarrow {}^4A_1$ components. The signs of the $^4A_2 \rightarrow {}^4E$ and $^4A_2 \rightarrow {}^4A_1$ transitions were opposite, and when they changed as a parameter was varied, they did so simultaneously. The ratio $R(E)/R(A_1)$ varied considerably, and the net $^4A_{2g} \rightarrow {}^4T_{2g}$ rotational strength could be made to change signs by variation of either geometric or electronic parameters.

Jensen has measured axial CD spectra of Λ-$[Cr(en)_3]^{3+}$ complexes in single crystals and concluded that the net CD results from a positive $^4A_2 \rightarrow {}^4E$ component and a negative $^4A_2 \rightarrow {}^4A_1$ component.[28] In D_3 symmetry the latter is forbidden by both electric and magnetic dipole selection rules when the incident light is parallel to the molecular axis, and Jensen has discussed how the axial CD spectrum can be resolved into the two spin-free components depending on the angle of incidence.[27,28]

Using eq 14 to calculate axial rotational strengths with $\zeta = 0$ reproduces these selection rules when the nitrogen and carbon coordinates are averaged to give 3-fold symmetry. However, when spin–orbit coupling is included, even to a small degree, the situation changes. Over the range of parameters tested, for light propagated parallel to the C_3 axis, we find that the four spin–orbit components of the $^4A_2 \rightarrow {}^4E$ transition consist of two pairs with opposite signs, while the two $^4A_2 \rightarrow {}^4A_1$ components have the same sign, which is opposite to that of the net $^4A_2 \rightarrow {}^4E$ $\Delta\epsilon$. Furthermore the signs of the (net) $^4A_2 \rightarrow {}^4A_1$ and $^4A_2 \rightarrow {}^4E$ peaks, as well as that for the combined $^4A_{2g} \rightarrow {}^4T_{2g}$ transition, change sign as ζ is increased. The net $\Delta\epsilon$ for the $^4A_2 \rightarrow {}^4E$ transition is calculated to be negative when the extent of spin–orbit coupling is small, switching to positive as ζ reaches about 100 cm^{-1}. At low values of ζ, the $^4A_2 \rightarrow {}^4A_1$ peak remains very weak, but grows with ζ until at $\zeta = 274$ cm^{-1} the individual components are approximately 10% of the size of the $^4A_2 \rightarrow {}^4E$ components. The contribution of the $^4A_2 \rightarrow {}^4A_1$ rotational strength to the total for the $^4A_2 \rightarrow {}^4T_2$ band is even larger, since sign cancellations reduce the contribution from the $^4A_2 \rightarrow {}^4E$ components.

The calculations just described refer to the axial CD spectrum of an idealized D_3 molecule. They confirm that spin-free selection rules can be usefully employed but that caution must be exercised as spin–orbit coupling becomes more important. Deviations from ideal D_3 symmetry damage the selection rules still further. Changing geometry from the symmetrized to the actual coordinates of Λ-$[Cr(en)_3]Cl_3$ (light still propagated along the average C_3 axis) results in the signs of all six $^4A_{2g} \rightarrow {}^4T_{2g}$ CD components being positive. At $\zeta = 274$ cm^{-1} all six components also are comparable in magnitude. There is no vestige of the selection rule against the $^4A_2 \rightarrow {}^4A_1$ transition. This may make it exceedingly difficult to calculate separate rotational strengths, $R(A_1)$ and $R(E)$, by using data from two different complexes.

The fact that the net $\Delta\epsilon$ of the $^4A_2 \rightarrow {}^4T_2$ transition from the axial single-crystal CD spectrum is about 10 times larger than that from the solution spectrum[28,33] may be viewed as supporting

(46) Kepert, D. L. *Inorganic Stereochemistry*; Springer-Verlag: West Berlin, 1982.

the conclusion that $R(E)$ and $R(A_1)$ have the same sign, with consequent reinforcement rather than the cancellation seen in solution.

Conclusions. Although there is a great deal of uncertainty about the conformational geometry of $[Cr(en)_3]^{3+}$ in solution and in a $2[Cr(en)_3]Cl_3 \cdot KCl \cdot 6H_2O$ host, the controversy generated by seemingly contradictory assignments for the $^2T_{1g}$ components in the two environments appears to be largely illusory. There is a high probability that both interpretations are correct. Assuming that the bite and twist angles are approximately the same in solution and in the solid state and that the *lel*$_2$*ob* conformational geometry obtains in both cases (although the nitrogen atoms are still assumed to have D_3 symmetry around the Cr in solution), a $^2T_{1g}$ splitting of approximately 150 cm^{-1} and a ^2E_g splitting of about 5 cm^{-1} are to be expected in solution. Since the two $^2T_{1g}$ peaks have opposite signs, a 150-cm^{-1} $^2T_{1g}$ splitting can easily be reconciled with the 300-cm^{-1} peak separation observed by Kaizaki[33] and by Richardson[23] in CD spectra. In the solid state, the deviations of the nitrogen atoms from D_3 symmetry lead to a larger ^2E_g splitting, but a smaller $^2T_{1g}$ splitting, as observed by Güdel.[25] In addition, the axial CD spectrum measured on single crystals results in positive signs for all five $\{^2E_g, ^2T_{1g}\}$ components, while the solution CD spectrum exhibits a mix of signs.

Acknowledgment. This material is based upon work supported in part by the National Science Foundation under Grant RII8610675. We also thank the donors of the Petroleum Research Fund, administered by the American Chemical Society, for their support of this research. I would also like to thank Prof. Lyle Parker for many enlightening discussions.

Contribution from the Chemistry Department, University of Canterbury, Christchurch 1, New Zealand, and Research School of Chemistry, Australian National University, P.O. Box 4, Canberra, ACT 2601, Australia

Vibrational Raman Spectra of Tris(1,2-ethanediamine) Complexes of Cobalt(III) and Rhodium(III)

Bryce E. Williamson,*[†] Lucjan Dubicki,*[‡] and Sven E. Harnung[§]

Received February 17, 1988

Polarized, single-crystal Raman spectra of the complexes $2[Co(en)_3]Cl_6 \cdot NaCl \cdot 6H_2O$ and $2[Rh(en)_3]Cl_6 \cdot KCl \cdot 6H_2O$ have been measured in the region 150–600 cm^{-1}. Assignments are made with the aid of a simplified normal-coordinate analysis calculation. The resonance Raman excitation profiles of $Co(en)_3^{3+}$ in the vicinity of the $^1T_1 \leftarrow {}^1A_1$ electronic transition have been reinvestigated, and the phenomenon of resonance deenhancement is confirmed. An analysis based on the error function model indicates that the observed deenhancement requires the displacements of the two interfering excited states to be in the *same* direction with respect to the ground state.

1. Introduction

Metal chelates of 1,2-ethanediamine (en) have been the subject of numerous investigations. In many cases they form uniaxial crystals that are suitable for a spectroscopic study of optical activity.[1,2] The metal chelates display extensive vibronic activity in the absorption,[1,3–7] emission,[6,7] and circular dichroism[1,3,4,6] spectra.

Although the vibrational spectra have been studied by many authors,[6,8–15] some of the assignments in the MN_6 skeletal region have remained controversial. Recently, a full normal-coordinate analysis of $Rh(en)_3^{3+}$ was made by Borch et al.[14–16] Unfortunately, their work contains errors in the E symmetry coordinates and some of the assignments of the E vibrations must be incorrect.

The Co(III) complexes of en[13] and other polyamine ligands, such as tacn[17] and sepulchrate,[17] exhibit deenhancement in the resonance Raman excitation profiles (RREP) of A_1 vibrations for excitation into the $^1T_1 \leftarrow {}^1A_1$ electronic transition. This effect has been interpreted as an interference between resonance scattering with the $^1T_1$ state and preresonance scattering from a charge-transfer state.[13,18] Previous analysis was restricted to the physically unrealistic case where only a single A_1 vibration was vibronically active and gave the result that the charge-transfer state was compressed along the A_1 coordinate.[18]

In this work we examine the skeletal vibrations of $Co(en)_3^{3+}$ and $Rh(en)_3^{3+}$ using polarized, single-crystal Raman spectroscopy. The symmetry coordinates are corrected, and a simplified normal-coordinate calculation is used to assign the vibrations. The resonance deenhancement of the RREP in $Co(en)_3^{3+}$ is confirmed. Contrary to earlier work,[18] we deduce that the charge-transfer state involved in preresonance scattering is expanded along the a_{1g} breathing coordinate.

2. Experimental Section

Preparation of Crystals. Crystals of (+)-$2[Co(en)_3]Cl_6 \cdot NaCl \cdot 6H_2O$ and (±)-$2[Co(en)_3]Cl_6 \cdot NaCl \cdot 6H_2O$, denoted hereafter as +Co and ±Co, respectively, were available from earlier studies.[1]

Two types of crystals of $Rh(en)_3^{3+}$ were examined spectroscopically, 15% (+)-$Cr(en)_3^{3+}$ and 1–2% (±)-$Cr(en)_3^{3+}$, both doped in the racemic host (±)-$2[Rh(en)_3]Cl_6 \cdot KCl \cdot 6H_2O$.

The 15% sample, denoted hereafter as ±Rh, was prepared by mixing 15.2 g of (+)-$[Rh(en)_3]Cl_3$ in 30 mL of H_2O and 15 g of (+)-$[Cr(en)_3]Cl_3$ in 35 mL of H_2O, at 50 °C. After cooling and filtration, the precipitate was washed with ice-cold H_2O. The precipitate, 29.8 g, and 16 g of (±)-$[Rh(en)_3]Cl_3$ were dissolved in 350 mL of H_2O at 35 °C, and 156 mL of saturated KCl, 452 mL of H_2O, and 32 mL of 4 M HCl were added. The filtered solution was placed in a thermostat at 32 °C. The

[†] University of Canterbury.
[‡] Australian National University.
[§] Chemistry Department I, University of Copenhagen, Denmark.

(1) Dubicki, L.; Ferguson, J.; Geue, R. J.; Sargeson, A. M. *Chem. Phys. Lett.* **1980**, *104*, 393–7.
(2) Dubicki, L.; Ferguson, J.; Williamson, B. *J. Phys. Chem.* **1984**, *88*, 4254–8.
(3) Dingle, R. *Chem. Commun.* **1965**, 304–5.
(4) Denning, R. G. *Chem. Commun.* **1967**, 120–1.
(5) Flint, C. D.; Mathews, A. P. *Inorg. Chem.* **1975**, *14*, 1219–20.
(6) Geiser, U.; Guedel, H. U. *Inorg. Chem.* **1981**, *20*, 3013–9.
(7) McCarthy, P. J.; Vala, M. T. *Mol. Phys.* **1973**, *25*, 17–34.
(8) Powell, D. B.; Sheppard, N. *Spectrochim. Acta* **1961**, *17*, 68–76.
(9) Krishnan, K.; Plane, R. A. *Inorg. Chem.* **1966**, *5*, 852–7.
(10) Gouteron-Vaissermann, J. *C. R. Seances Acac. Sci., Ser. B* **1972**, *275*, 149–50.
(11) James, D. W.; Nolan, M. J. *Inorg. Nucl. Chem. Lett.* **1973**, *9*, 319–29.
(12) Gouteron, J. *J. Inorg. Nucl. Chem.* **1976**, *38*, 63–71.
(13) Stein, P.; Miskowski, V.; Woodruff. W. H.; Griffin, J. P.; Werner, K. G.; Gaber, B. P.; Spiro, T. G. *J. Chem. Phys.* **1976**, *64*, 2159–67.
(14) Borch, G.; Klaboe, P.; Nielsen, P. H. *Spectrochim. Acta, Part A* **1978**, *34A*, 87–91.
(15) Borch, G.; Gustavsen, J.; Klaboe, P.; Nielsen, P. H. *Spectrochim. Acta, Part A* **1978**, *34A*, 93–99.
(16) Borch, G.; Nielsen, P. H.; Klaboe, P. *Acta Chem. Scand., Ser. A* **1977**, *A31*, 109–19.
(17) Williamson, B. E.; Dubicki, L., unpublished results.
(18) Zgierski, M. Z. *J. Raman Spectrosc.* **1977**, *6*, 53–6.

0020-1669/88/1327-3484$01.50/0